Millimeter-Wave Dual-Band Microstrip Patch Antennas Using Multilayer GaAs Technology

David Sánchez-Hernández, Q. H. Wang,
Ali A. Rezazadeh, and Ian D. Robertson

Abstract—**This paper describes the performance and construction of several multiband integrated microstrip antennas around 35 GHz on in-house semi-insulating multilayer GaAs. The simulated and measured input impedances and radiation patterns at both the lower and upper resonant frequencies are given and some experimental results are provided to check the accuracy of the electromagnetic simulations.**

I. Introduction

Recently, the use of microstrip antennas somehow modified to act as dual-band elements has received much attention [1]. Multilayer stacked patch antennas have enjoyed increasing support as multiband antennas for use in systems where weight, cost, and conformability are critical factors. Other techniques to widen the bandwidth of patch antennas have also been studied [2], [3] and are starting to challenge the stacked configuration, especially due to their reduction in size. The dream of entire receiver subsystems on a chip, or even complete transceivers, make the mm-wave region and the monolithic microwave integrated circuit (MMIC) technology development the key factor. Designers must not only integrate the antenna and its associated circuits, but also phase shifters, amplifiers, and control circuits. The reason to build these intelligent antennas monolithically is largely based upon the fact that it would be practically impossible to achieve better results otherwise. Monolithic active antennas elements fabricated in a single, high resolution, integrated circuit process can provide both better reliability and reproducibility in comparison to their hybrid counterparts. Previous investigations [4] lead to the conclusion that microstrip antenna arrays will be useful up to a frequency of 100 GHz, where it should be possible to design microstrip antenna arrays with adequate gain, good pattern quality, low VSWR and acceptable efficiency. Hence, very good electrical performance combined with very reasonable electric weight would make these antennas excellent candidates for new types of communications, precision radar, radio astronomy and remote sensing systems, including video distribution, secure communications systems, meteorological monitoring, aircraft-to-satellite communication and imaging array antennas.

This paper describes the performance and construction of several multiband integrated microstrip antennas operating around 35 GHz on in-house semi-insulating multilayer GaAs. The simulated and measured input impedances and radiation patterns at both the lower and upper resonant frequencies are given and some experimental results are provided to check the accuracy of the electromagnetic simulations.

Manuscript received November 10, 1995; revised May 24, 1996. This work was supported in part by the EEC under the Training and Mobility of Researchers Programme (IV Framework) and by the Engineering and Physical Sciences Research Council.

D. Sánchez-Hernández and I. D. Robertson are with the Centre for Telecommunications Research, Department of Electronic and Electrical Engineering, King's College, University of London, Strand, London WC2R 2LS, U.K.

Q. H. Wang and A. A. Rezazadeh are with the Physical Electronics Research Group, Department of Electronic and Electrical Engineering, King's College, University of London, Strand, London WC2R 2LS, U.K.

Publisher Item Identifier S 0018-9480(96)06390-9.

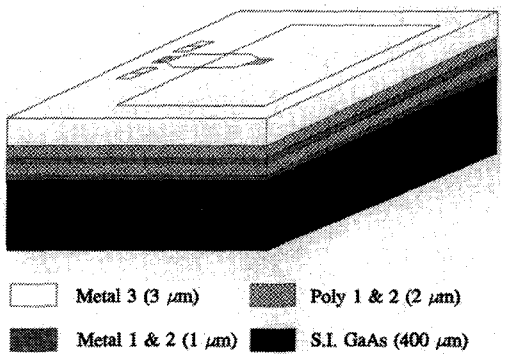

Fig. 1. Multilayer structure on the GaAs substrate and layout of single patch antenna.

II. Microstrip Patch Antenna Elements

The selected substrate configuration is composed of five layers as shown in Fig. 1. The diverse MMIC's were fabricated at King's College using a 400-μm-thick GaAs substrate with a dielectric permittivity of 12.85. The first, third, and fifth layers are metal with a thickness of 1 μm, 1 μm, and 3 μm, while the second and fourth layers are PIQ-13 (Hitachi) polymides with a thickness of 2 μm. The different circuit layers can be interconnected through a polymide insulating layer window. After substrate cleaning and preheating, the polymide films were created by spin coating at 3200 rpm for 40 sec, which gives a PIQ thickness of around 2.0 μm with a deviation of ± 0.1 μm. The interconnection windows were achieved by Reactive Ion Etching (RIE) through a AZ1529 photoresist layer patterned using lithography. Different polymide etching conditions were tested, including changing plasma power, chamber pressure, and gas flow rate. Planarizations effects on any surface features were also tested. Metal layers were formed by lift-off techniques. Four different elements were designed and fabricated. Two single patch antennas were simulated and built in metals 2 and 3 as references. The feedlines were placed on metal 1. The layout of these single patch antennas is depicted in Fig. 1. Two different dual-band designs were also constructed; a stacked patch antenna using metals 2 and 3 and a spur-line antenna in metal 2. Assuming that the patches are cocentered, impedance equalization is possible at the two resonant frequencies by choosing the top patch slightly shorter than the bottom patch. Introducing some offset enables a better adjustment of coupling effects, and hence a wider bandwidth, but the structural dissymmetry can create some depointing in the E-plane [5]. Hence both dimensions of the patch are modified while keeping the feedpoint location. With a smaller parasitic patch, a large frequency separation between the two resonant frequencies and a wider bandwidth can be achieved. The presence of a parasitic director, however, is expected to slightly reduce the resonant frequency of the lower patch antenna as it will be commented further on. Additionally, a dual-band spur-line patch antenna was built as shown in Fig. 2. In this figure the length of the spur a and the gap b determine the center frequency f_0 given by

$$a = \frac{2.997\,925\ 10^8}{4 f_0 \sqrt{K_{\text{effo}}}} - \Delta l_1 \tag{1}$$

where K_{effo} and Δl_1 are the odd-mode effective dielectric constant and the effective length extension due to the gap b, respectively. Δl_1 can be calculated by

$$\Delta l_1 = C_{\text{odd}} V_{\text{po}} Z_{\text{oo}} \tag{2}$$

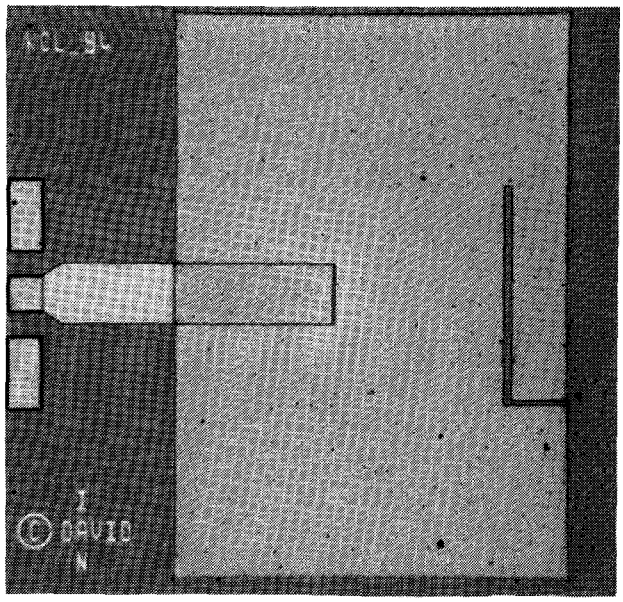

Fig. 2. Microphotograph of spur-line antenna.

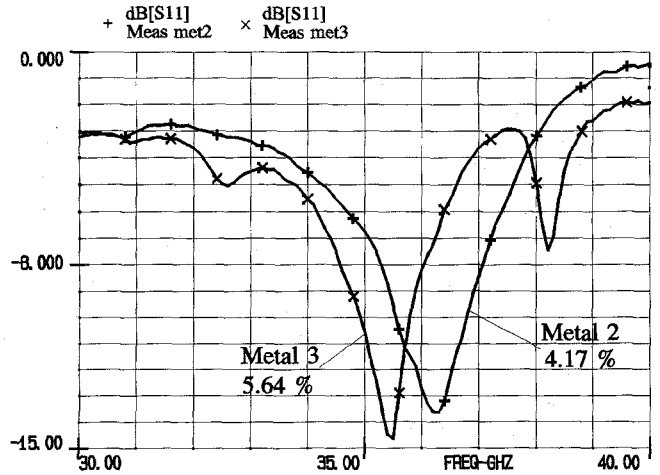

Fig. 3. Measured input return loss for single patches on metals 2 and 3.

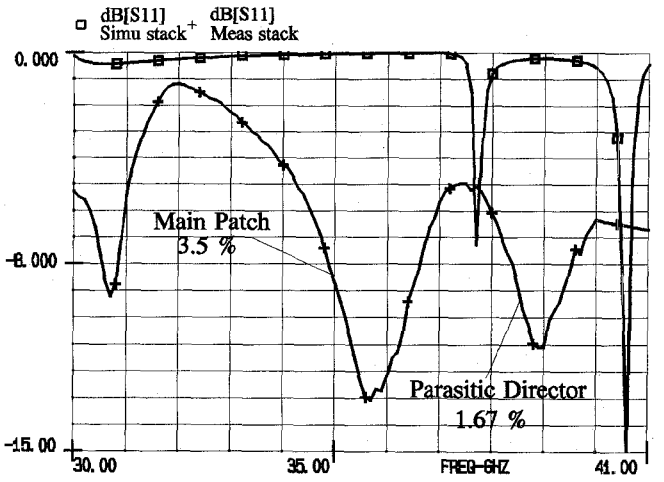

Fig. 4. Simulated and measured input return loss for the stacked patch antenna.

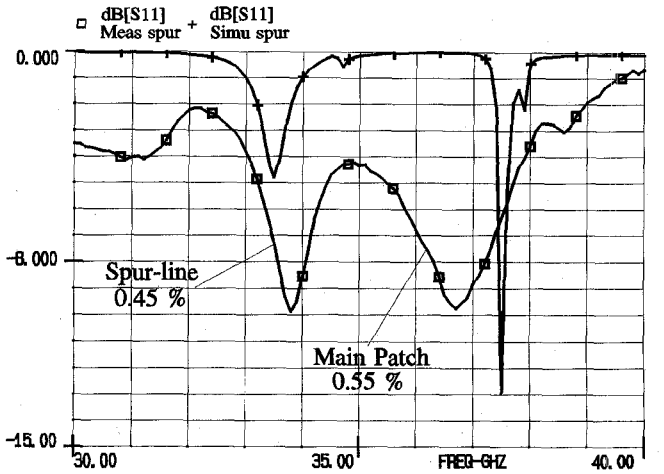

Fig. 5. Simulated and measured input return loss for the spur-line patch antenna.

where V_{po} is the phase velocity of the odd mode, C_{odd} is the resulting capacitance of an antisymmetrically excited two-port network of the π-network model for a gap in a microstrip line and can be calculated by modifying Benedek's analysis [6] because at resonance no current flows along the gap. Thus

$$C_{\mathrm{odd}} = C_1 + 2C_{12} \tag{3}$$

where the expressions for the different capacitances can be found in [7]. The coupled lines of the filter must be embedded and centered in the radiating edge of the patch opposite the feed point. A polymide insulating window was used to interconnect the feedline and the patch at the desired feedpoint for all elements. This choice is based upon the fact that while in probe-fed patches both the co- and cross-polar patterns are slightly deformed, on the other hand with aperture-coupled structures the copolar component exhibits some depointing, which is stronger in the upper portion of the passband. There are other reasons. Slot-coupled feed configurations are more sensitive to misalignments of the resonators and exhibit a certain amount of backscattering radiation, which is nonexistent in coaxially-fed antennas.

III. Theory

Analysis of these antennas is based on integral equations solved in the spectral domain using the method of moments (MoM). The boundary value problem for the unknown surface current is expressed in terms of a mixed potential integral equation

$$E_t^i(r) = Z_S J_S(r) + jw \int_S \bar{G}_A(r \mid r') J_S(r') d'S - \frac{1}{jw} \Delta t \int_S G_V(r \mid r') \Delta t J_s(r') d'S \tag{4}$$

where E_t^i is the incident electric field tangent to the conductive surfaces, J_S is the unknown surface current, G_A is a three-dimensional (3-D) dyadic Green's function, G_V is the Green's function associated with the scalar potential and Z_s is the surface impedance that accounts for the finite conductivity of the patch. The unknowns in (4) are the surface currents J_s. This mixed potential equation is a Fredholm integral equation of the second kind. The far fields are obtained using a superposition integral over the patch with the asymptotic forms

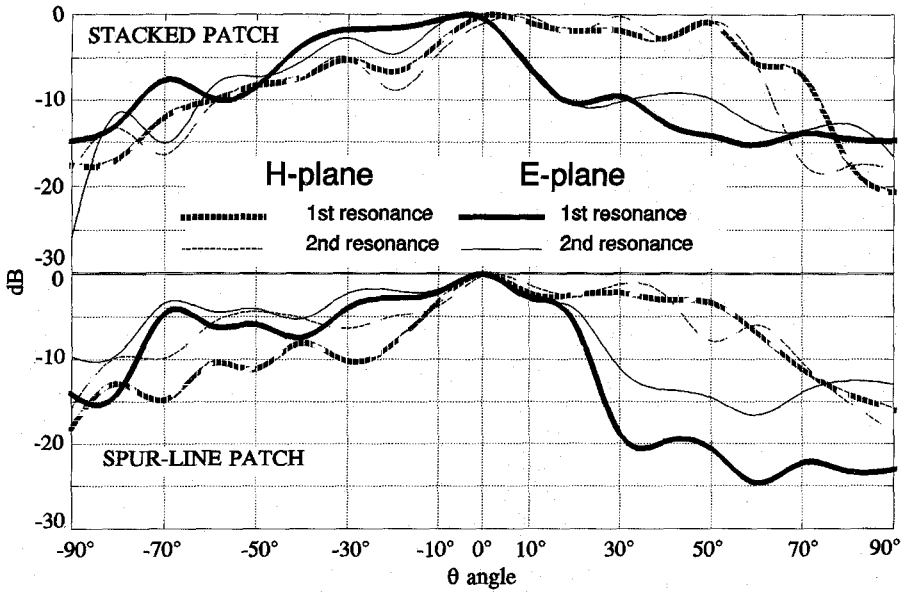

Fig. 6. Measured radiation patterns for the dual-band monolithic antennas.

of the Green's functions in the far field. The commercial package *em* by Sonnet Software was selected to model the structures. *Em* is a practical electromagnetic analysis tool which can calculate *S*-parameters for predominantly planar 3-D structures at all frequencies. The analysis is "full-wave," taking into account a wide variety of possible electromagnetic effects, including dispersion, discontinuities, package effects, moding, and losses for both metal and dielectrics. *Em* analyzes planar structures inside a shielding box. The feed point in the patch can be created by a via to ground which allows z-directed currents. Then the ground end of that via has to be specified as a port. This is a simple model of a microstrip coaxial feed. In other words, the voltage gap put across the ground has parasitics that are not calibrated. However, for moderately thin substrates the quality factor, Q, of the printed antenna is very high. Hence the currents in such case on the patch element dominate those of the feed, and the simple feed model has proven to be accurate enough.

IV. Simulated and Measured Results

The VSWR of the different antennas for the different resonances were measured using a Summit 9000 probe station connected to a HP8510B network analyzer. Measurements of the MMIC's radiation patterns were achieved with a mounting fixture. Fig. 3 shows the measured input reflection coefficient for the single patches in metal 2 and 3. The measured VSWR bandwidth for the patch in metal 2 was 4.17% (1.5 GHz at $f_0 = 36$ GHz), while that of the patch in metal 3 was 5.64% (2 GHz at $f_0 = 35.45$ GHz). It can be observed from Fig. 3 that a low dielectric permittivity superstrate affects the input impedance, increasing the resonant frequency and reducing the bandwidth. This could appear to be in contradiction to other studies, where a dielectric superstrate on a patch decreases the resonant frequency [8]. However, with a closer study of this case, it was found that the increase was due to the different metallization thickness of the metals. As demonstrated in other investigations [9], an increase of metallization thickness lowers the fundamental resonant frequencies of the patch. This will also affect other structures. Ripples detected in all the measured patterns are attributable to the finiteness of the substrate and due to the fact that the patches were on 2 mm^2 diced chips. Simulated radiation patterns from *em* could not be obtained due to the fact that patgen (pattern generation programme for *em*) has to perform the analysis for single-layer open environment with a substrate of infinite or very large extent. The computed and measured input impedances for the stacked patch and the spur-line patch can be seen in Figs. 4 and 5. Their radiation patterns are shown in Fig. 6. The crosspolarization levels were 15 dB down from the copolar power levels. The measured bandwidth for the multilayer patch was 3.5% (1.25 GHz at $f_{01} = 35.65$ GHz) and 1.67% (650 MHz at $f_{02} = 38.9$ GHz). This means an increase of 1% with respect to the single patch in metal 2, where the main patch of the stacked configuration is placed. Both resonant frequencies are lower than the expected ones. This is due to the *em* assumption of zero-thickness metallizations, with the consequent decrease of resonant frequencies as abovementioned. Moreover, it is also known that the presence of the parasitic director reduces the resonant frequency of the patch. Additionally, it is known that the impedance of the antenna at the upper resonance is very sensitive to the ε_r and thickness of the upper dielectric. Hence, the actual ± 0.1 μm deviation on the PIQ thickness also has an effect on the resonant frequency. At the same time, the effect of the superstrate produces a notch around 30 GHz on the stacked patch. This notch disappears with the spur-line configuration. With this spur-line technique the measured bandwidth was found to be 0.45% (150 MHz at $f_{01} = 33.75$ GHz) and 0.55% (200 MHz at $f_{02} = 36.75$ GHz). This bandwidth is lower in frequency than that of the stacked configuration, but important advantages can be obtained instead. First, due to its inherent behavior, the spur-line patch not only produces a first resonance considerably lower than the first resonance of the stacked patch, but also uses the same area. To obtain the same lower resonant frequency with a multilayer patch an additional 50% area would be needed. This greater area needed for the patch would lead to stronger coupling and a more complex design and layout of the active devices. Since the notch around 30 GHz disappears in the spur-line antenna, there is no power launched to this undesired excited mode.

These results also demonstrate that, with these structures, a large separation between the two resonant frequencies with good matching in both of them could be achieved. In Fig. 6, the stacked patch does not exhibit perfect symmetry, pointing to the geometrical alignment problem mentioned before. We also observe in Fig. 6 a slightly

deformed E-plane, which confirms the effect of transverse currents on the E-plane rather than on the H-plane.

V. Conclusion

With the examples provided here it has been shown that dual-band elements can be designed for use on monolithic GaAs active antennas, with planar configurations offering improved characteristics compared to stacked elements. The alliance of monolithic device technology and printed-circuit antennas has opened an unlimited number of possibilities for both antenna and system designer. Technology has been developed for 90 GHz systems, but higher operating frequencies for new communication systems are coming fast, and research is even moving toward the 1 THz region [10]. Likewise, new materials such as InP will play an important role. A combination of different permittivities on the same substrate, say, small islands of high dielectric constant material on a low dielectric constant substrate could be an important option to overcome the diverse problems encountered when trying to integrate microstrip antennas with acvtive circuits.

References

[1] P. Piazzesi *et al.*, "Dual-band dual-polarized patch antennas," *Int. J. Microwave and Millimeter-Wave Computer-Aided Eng.*, vol. 5, no. 6, pp. 375–384, 1995.

[2] D. Sánchez-Hernández and I. D. Robertson, "Analysis and design of a dual-band circularly polarized microstrip patch antenna," *IEEE Trans. Antennas Propagat.*, vol. 43, no. 2, pp. 201–205, 1995.

[3] F. Croq and D. M. Pozar, "Multifrequency operation of microstrip antennas using aperture coupled parallel resonators," *IEEE Trans. Antennas Propagat.*, vol. 40, no. 11, pp. 1367–1374, 1992.

[4] F. K. Schwering, "Millimeter wave antennas," *IEEE Proc.*, 1992, vol. 80, no. 1, pp. 92–102.

[5] J. P. Damiano *et al.*, "Dual frequency and offset multilayer microstrip antennae," in *8th IEE Int. Conf. Antennas Propagat.*, pp. 372–375.

[6] P. Benedek and P. Silvester, "Equivalent capacitances for microstrip gaps and steps," *IEEE Trans. Microwave Theory Tech.*, vol. 20, pp. 729–733, 1972.

[7] J. R. James and P. S. Hall, *Handbook of Microstrip Antennas*, M. Haneishi and Y. Suzuki, Eds. London: Peter Peregrinus, vol. 1, 1989, p. 231.

[8] A. Bhattacharyya and T. Tralman, "Effects of dielectric superstrate on patch antennas," *Electron. Lett.*, vol. 24, no. 6, pp. 356–358, 1988.

[9] T.-S. Horng *et al.*, "The influence of metallization thickness on a microstripline-fed patch antenna," in *IEEE Antennas Propagat. Int. Symp. Dig.*, 1994, pp. 940–943.

[10] S. Lucyszyn, Q. H. Wang, and I. D. Robertson, "0.1 THz rectangular waveguide on GaAs semi-insulating substrate," *Electron. Lett.*, vol. 31, no. 9, pp. 721–722, 1995.

Planar Millimeter-Wave Antennas Using SiN_x-Membranes on GaAs

M. Stotz, G. Gottwald, H. Haspeklo, and J. Wenger

***Abstract*—Planar aperture coupled microstrip antennas for 77 GHz are demonstrated for the first time. As far as possible standard GaAs monolithic microwave/millimeter-wave integrated circuit (MMIC) technology is used to realize the antennas. The antenna patches are suspended on a thin dielectric SiN_x membrane on GaAs substrate. Therefore a novel plasma-enhanced chemical vapor deposition (PECVD) process step for the fabrication of the membranes is developed and described. The single antenna patches are coupled to a microstrip line through an aperture in the ground metallization. The method of moments in spectral domain is applied to design the patches. The feed network of a 3×1 antenna array for homogeneous excitation is simulated and optimized with a microwave design system (MDS). From reflection measurements the operation frequency of this triple patch antenna is determined to be 77.6 GHz. The farfield antenna characteristics are measured in an anechoic chamber, showing good agreement between simulated and measured results and a co- to cross-polarization isolation better than 30 dB.**

I. Introduction

Over a period of more than 25 years the development of microstrip and aperture coupled patch antennas has emerged as a major activity within the antenna field. The interest in these antenna types lies in their advantages such as low cost, mass production, lightweight, conformity to surface, and dual polarization capability. Especially at millimeter-wave frequencies the occupied area on the substrate becomes small enough, so that it can directly be integrated with microwave integrated circuits. When using semiconductor materials (Si or GaAs) as dielectric substrates for antennas the relatively high permittivity ($\varepsilon_r \approx 12 \cdots 13$) is disadvantageous due to the reduced radiation efficiency. Therefore technological measures have to be taken to reduce the effective ε_r to reasonable low values. One means is, to etch many closely spaced via-holes under the antenna patch or to reduce the thickness of the substrate locally under the patches to obtain a decreased ε_r [1], [2]. Another possibility is the use of thin membranes fabricated on Si or GaAs by using SiO_2 and/or SiN_x. On Si substrates this technique has been intensively used in [3]–[6] for the fabrication of antennas, detectors, and filters for frequencies well up into the submillimeter-wave range.

This communication describes a novel approach to realize planar antennas for automotive radar sensors for 77 GHz (e.g., autonomous intelligent cruise control, collision avoidance, or road surface detection). The realization of 3×1 antenna arrays suspended on thin, large, and stable SiN_x membranes on GaAs substrate is reported for the first time. In the following the design steps of the aperture coupled patches, the process procedures for the fabrication of the membranes compatible with the MMIC technology, as well as the measured performance of the antenna array are described.

II. Design

For the radiating element the aperture coupling antenna concept is chosen (Fig. 1). Despite the necessity of multilayer fabrication

Manuscript received November 10, 1995; revised May 24, 1996.

M. Stotz was with Daimler-Benz Research Center, High Frequency Electronics, D-89081 Ulm, Germany. He is now with TH Darmstadt, Institut für Hochfrequenztechnik, D-64283 Darmstadt, Germany.

G. Gottwald, H. Haspeklo, and J. Wenger are with Daimler-Benz Research Center, High Frequency Electronics, D-89081 Ulm, Germany.

Publisher Item Identifier S 0018-9480(96)06391-0.